© 2017. Published by The Company of Biologists Ltd | Journal of Cell Science (2017) 130, 2306-2316 doi:10.1242/jcs.198390

RESEARCH ARTICLE

Localisation of Nup153 and SENP1 to nuclear pore complexes is required for 53BP1-mediated DNA double-strand break repair

Vincent Duheron*, Nadine Nilles*, Sylvia Pecenko, Valérie Martinelli and Birthe Fahrenkrog‡

ABSTRACT

The nuclear basket of nuclear pore complexes (NPCs) is composed of three nucleoporins: Nup153, Nup50 and Tpr. Nup153 has a role in DNA double-strand break (DSB) repair by promoting nuclear import of 53BP1 (also known as TP53BP1), a mediator of the DNA damage response. Here, we provide evidence that loss of Nup153 compromises 53BP1 sumoylation, a prerequisite for efficient accumulation of 53BP1 at DSBs. Depletion of Nup153 resulted in reduced SUMO1 modification of 53BP1 and the displacement of the SUMO protease SENP1 from NPCs. Artificial tethering of SENP1 to NPCs restored non-homologous end joining (NHEJ) in the absence of Nup153 and re-established 53BP1 sumoylation. Furthermore, Nup50 and Tpr, the two other nuclear basket nucleoporins, also contribute to proper DSB repair, in a manner distinct from Nup153. Similar to the role of Nup153, Tpr is implicated in NHEJ and homologous recombination (HR), whereas loss of Nup50 only affects NHEJ. Despite the requirement of all three nucleoporins for accurate NHEJ, only Nup153 is needed for proper nuclear import of 53BP1 and SENP1-dependent sumoylation of 53BP1. Our data support the role of Nup153 as an important regulator of 53BP1 activity and efficient NHEJ.

KEY WORDS: Nuclear pore complex, Nucleoporin, Nup153, 53BP1, SUMO, SENP1, DNA damage response

INTRODUCTION

Nuclear pore complexes (NPCs) are gates for all molecular trafficking between the cytoplasm and the nucleus of interphase eukaryotic cells. NPCs consist of multiple copies of ∼30 different nucleoporins (Nups) (Cronshaw et al., 2002; Ori et al., 2013; Rout et al., 2000; for reviews, see Dickmanns et al., 2015; Kabachinski and Schwartz, 2015) resulting in an overall complex of ∼110 MDa in vertebrates (Ori et al., 2013; Reichelt et al., 1990). On the nuclear side of the NPCs, eight filaments emanate to form the nuclear basket, which is primarily composed of the nucleoporins Nup153, Nup50 and Tpr (Beck et al., 2004, 2007; Duheron et al., 2014; Fahrenkrog and Aebi, 2003; Frenkiel-Krispin et al., 2010; Lim et al., 2008; Maimon et al., 2012; Ori et al., 2013). All three basket nucleoporins are important players in nucleocytoplasmic transport (Dickmanns et al., 2015) and are evolutionarily conserved, with functional homologues in yeast, *Drosophila*, *Xenopus* and other species (Bogerd et al., 1994; De Souza et al., 2009; Dilworth et al., 2001, 2005; Kosova et al., 2000; Strambio-de-Castillia et al., 1999).

Laboratory Biology of the Nucleus, Institute for Molecular Biology and Medicine, Université Libre de Bruxelles, Charleroi 6041, Belgium.
*These authors contributed equally to this work

‡Author for correspondence (bfahrenk@ulb.ac.be)

V.D., 0000-0002-4319-4074; B.F., 0000-0003-4080-9413

Received 10 October 2016; Accepted 28 May 2017

Recent years have provided increasing evidence that nucleoporin function exceeds nucleocytoplasmic transport and that they directly or indirectly control aspects of DNA-based processes, such as DNA transcription, replication and repair (Gay and Foiani, 2015; Géli and Lisby, 2015; Ibarra and Hetzer, 2015). In this context, it has been shown that Nup153 mediates the nuclear import of the DNA repair mediator 53BP1 (also known as TP53BP1), regulating the non-homologous end joining (NHEJ) pathway of DNA double-strand break (DSB) repair (Cobb et al., 2016; Lemaitre et al., 2012; Moudry et al., 2011). Nup50 appears to be required for the nuclear import of XRCC1, which plays roles in single-strand break and base excision repair (Kirby et al., 2015). So far nothing is known about a putative role for Tpr in the DNA damage response (DDR), but yeast cells lacking Mlp1 and Mlp2, the yeast homologue of Tpr (Strambio-de-Castillia et al., 1999), accumulate DNA damage and are highly sensitive to damaging drugs (Hediger et al., 2002; Palancade et al., 2007; Zhao et al., 2004). The role of Mlp1 and Mlp2 in DDR is not well characterised, but appears to be linked to their anchor function of the yeast SUMO-protease Ulp1 (Palancade et al., 2007; Zhao et al., 2004). Small ubiquitin-like modifiers (SUMOs) are proteins that are covalently conjugated to a large set of target proteins, thereby altering their activity (Flotho and Melchior, 2013; Mukhopadhyay and Dasso, 2007). Ulp1 belongs to a family of cysteine proteases that specifically target SUMOs to reverse their action (Mukhopadhyay and Dasso, 2007; Yeh, 2009). The closest mammalian homologous of Ulp1 are the two SUMO-specific proteases 1 and 2 (SENP1 and SENP2). SENP1 and SENP2 are nuclear proteins that harbour nuclear localisation signals (NLSs) as well as nuclear export signals (NESs) (Bailey and O'Hare, 2004; Gong et al., 2000; Itahana et al., 2006; Kim et al., 2005; Yeh, 2009). They associate with NPCs and are concentrated at the nuclear basket, where they dynamically and primarily interact with Nup153 (Chow et al., 2012; Hang and Dasso, 2002; Zhang et al., 2002). No interaction of SENP2 with Tpr has been found (Zhang et al., 2002), but SENP2 expression was reduced in HeLa cells depleted for Tpr (David-Watine, 2011). Delocalisation of Ulp1 from NPCs causes DNA damage and cell cycle defects, phenotypes attributed to inappropriate desumoylation of nucleoplasmic target proteins that are normally protected from Ulp1 (Nie and Boddy, 2015; Palancade et al., 2007; Zhang et al., 2002). Similarly, it has been shown that a mutant form of SENP2 that is unable to interact with Nup153 more effectively promotes desumoylation (Hang and Dasso, 2002), indicating that NPCs in fact play important roles in spatially restricting the activity of SUMO protease.

Here, we provide evidence that displacement of SENP1 from NPCs in cells depleted for Nup153 affects sumoylation of 53BP1 and reduces the efficiency of DSB repair by NHEJ.

RESULTS

Depletion of nuclear basket nucleoporins alters the DDR

It has previously been shown that the depletion of Nup153 by use of small interfering RNAs (siRNAs) sensitised cells to DNA

Journal of Cell Science

Journal of Cell Science (2017) 130, 2306-2316 doi:10.1242/jcs.198390

DSB-inducing agents (Lemaitre et al., 2012; Moudry et al., 2011). To address the question of whether or not Nup50 and Tpr, the two partners of Nup153 at the NPC nuclear basket, are also involved in DSB repair, we analysed the effect of their depletion for clonogenic survival of U2OS cells after exposure to genotoxic stress. As shown in Fig. 1A and Table 1, U2OS cells depleted for Nup153 and Tpr, respectively, exhibited a slight increased sensitivity to the radiomimetic drug neocarzinostatin (NCS) and a trend towards decreased viability as compared to Nup50-depleted cells and control cells transfected with scrambled non-targeting (NT) siRNAs. This decreased viability was statistically relevant for Nup153-depleted cells when treated with 2 µg/ml NCS (Fig. 1B). The efficiency of the silencing of the three nucleoporins was verified by immunofluorescence microscopy and western blot analyses (Fig. S1A,B). Next, we sought to directly test which pathway for DSB repair was affected by the respective depletion of Nup153 and Tpr. To this end, we utilised cell lines that were co-transfected with siRNAs and GFP reporter constructs to monitor the efficiency of NHEJ (Seluanov et al., 2004) and homologous recombination (HR) (Pierce et al., 1999), respectively. To monitor NHEJ efficiency, U2OS cells were depleted for the particular nucleoporin, transfected with a linearised pEGFP-Pem1-Ad2 plasmid and analysed by flow cytometry (see Materials and Methods). As shown in Fig. 1C, depletion of either of the three nuclear basket nucleoporins decreased NHEJ efficiency as compared to that seen in control cells (normalised to 1), similar to what is observed in 53BP1-depleted cells. To monitor HR, the recombination substrate DR-GFP was utilised, in which a gene conversion event results in the expression of an intact GFP protein, and assessed by flow cytometry (see Materials and Methods). Similar to what is seen upon depletion of Rad51 in U2OS cells, cells lacking Nup153 and Tpr, respectively, were less competent for HR as compared to

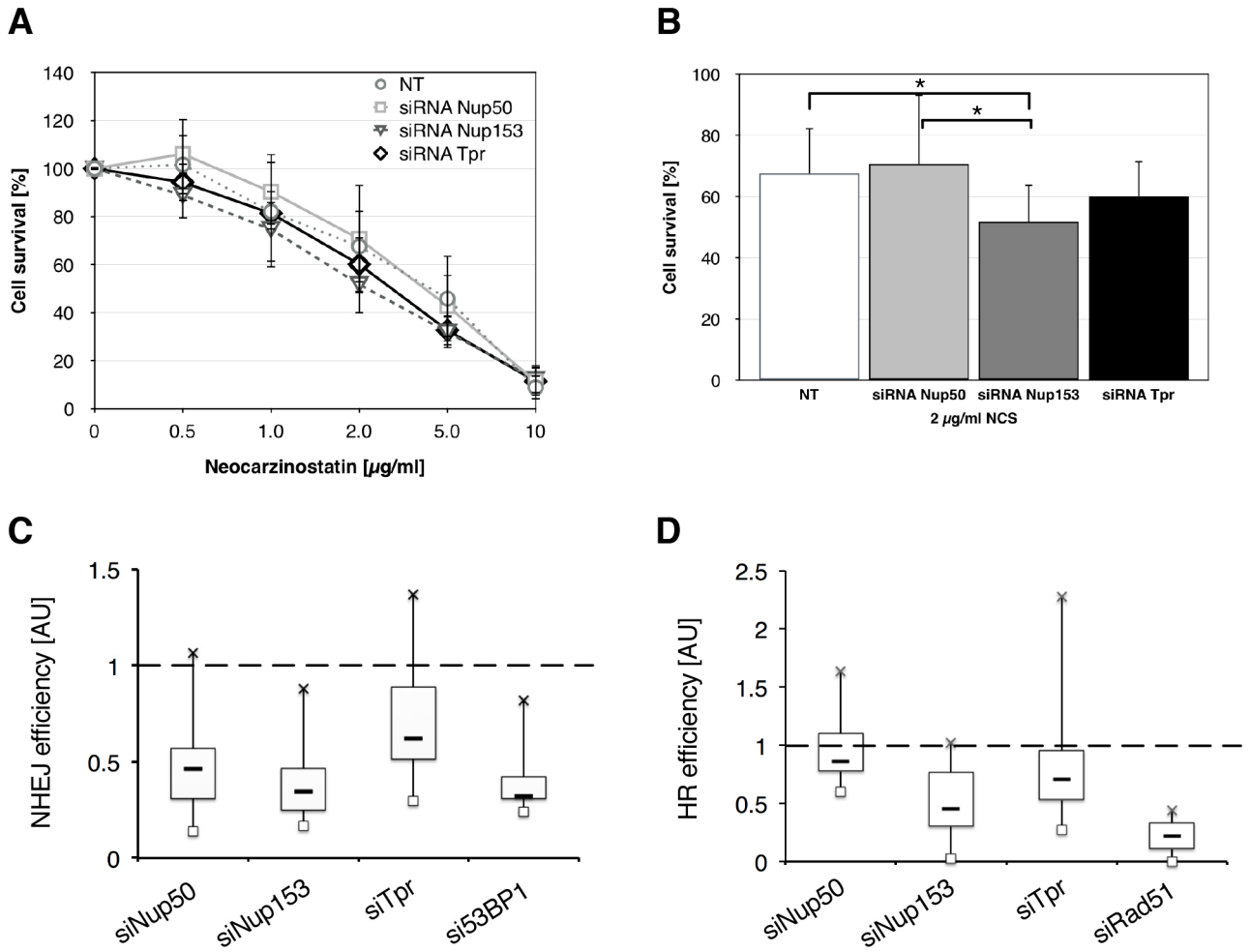

Fig. 1. Depletion of Nup153 and Tpr from U2OS cells leads to decreased efficiency of DNA DSB repair. (A) Clonogenic survival assay of U2OS cells treated with the indicated siRNAs, followed by exposure to increasing concentrations of the radiomimetic drug neocarzinostatin (NCS). U2OS cells were counted 72 h after transfection, seeded in triplicates in 6-well plates (1000 cells per well), and treated with NCS at the indicated concentrations for 15 min. Cells were allowed to form colonies for 10 days. Nup153- as well as Tpr-depleted cells exhibited increased sensitivity to NCS, as compared to Nup50-depleted and control cells. Survival was normalised to untreated control cells. (B) Clonogenic survival assay of U2OS cells treated with the indicated siRNAs, followed by exposure to 2 µg/ml NCS. The survival of Nup153-depleted cells was significantly reduced as compared to control and Nup50-depleted cells. Data in A and B are mean±s.d. from three independent experiments. NT, non-targeting siRNA. *P<0.05 (t-test, one-tailed). (C) NHEJ efficiencies in U2OS cells treated with the indicated siRNAs. NHEJ efficiency was monitored by co-transfection of linearised pEGFP-Pem1-Ad2 and analysis by flow cytometry. NHEJ efficiency for nucleoporin-depleted cells was quantified relative to that in control cells (value set at 1) for 150,000 cells from ten independent experiments. (D) HR efficiencies in U2OS cells stably expressing the HR reporter construct and treated with the indicated siRNAs was analysed by flow cytometry. HR efficiency for nucleoporin-depleted cells was quantified relative to control cells (value set at 1) for 135,000 cells from nine independent experiments. The box plots in C and D represent the 25–75th percentiles, and the median is indicated. Whiskers show 1.5× the interquartile range above or below the data. Outliers are not shown. AU, arbitrary units.

Journal of Cell Science (2017) 130, 2306-2316 doi:10.1242/jcs.198390

Table 1. Clonogenic survival of U2OS cells after siRNA and NCS treatment

	0 µg/ml NCS	0.5 µg/ml NCS	1 µg/ml NCS	2 µg/ml NCS	5 µg/ml NCS	10 µg/ml NCS
siRNA NT	100±0	101.7±12.5	82.0±20.8	67.6±14.9	45.8±17.9	8.9±5.1
siRNA Nup50	100±0	106.1±14.6	90.3±15.9	70.7±22.7	42.8±13.0	11.2±6.0
siRNA Nup153	100±0	88.9±9.6	74.7±15.9	51.8±12.1	31.9±6.7	12.3±5.8
siRNA Tpr	100±0	94.3±7.9	81.4±4.8	60.1±11.5	32.7±6.3	11.4±6.1

Results are the mean±s.d. percentage survival for three independent experiments.

Nup50-depleted and control cells (Fig. 1D). Taken together, these data indicate that in particular Nup153 and Tpr are implicated in DNA DSB repair.

Localisation of 53BP1 is only affected by depletion of Nup153

Previously it has been demonstrated that Nup153 is involved in the nuclear import of 53BP1 (Moudry et al., 2011). We therefore next asked whether the depletion of Nup50 and Tpr also affects 53BP1 nuclear import. By performing immunofluorescence analyses, we found, however, that only down-regulation of Nup153 reduced the nuclear accumulation of 53BP1 (Fig. 2A,B), while the overall expression levels of 53BP1 remained unchanged (Fig. 2D).

Having seen that cells lacking Nup153 or Tpr are also less competent at HR, we wondered whether BRCA1 nuclear localisation would be altered by the depletion of these two nucleoporins. In control cells, BRCA1 was mainly present in the nucleus, but a small proportion was also detected in the cytoplasm (Fig. 2A). This distribution of BRCA1 did not change upon the respective down-regulation of Nup153, Nup50 and Tpr in U2OS cells (Fig. 2A,C) as was also the case for BRCA1 expression levels (Fig. 2E). Taken together, our data indicate that general nuclear import defects are unlikely to be the exclusive cause for impaired DSB repair in cells lacking nuclear basket components.

Nup153 and Tpr are required for the dissolution of repair foci

We next analysed the behaviour of 53BP1 and BRCA1 in U2OS cells lacking Nup153, Nup50 and Tpr, respectively, after the induction of DSBs by NCS (50 ng/ml for 15 min). We monitored the formation of 53BP1 and BRCA1 foci at DSBs and their dissolution over time. As shown in Fig. 3A, the particular downregulation of the nuclear basket nucleoporins did not impair 53BP1 and BRCA1 foci formation after NCS treatment, although more 53BP1 was detectable in the cytoplasm of Nup153-depleted cells. In control cells, the number of BRCA1 (Fig. 3B) and 53BP1 (Fig. 3C) foci increased during the first 2 h after NCS treatment and then progressively decreased. The decrease in foci number was accompanied by an increase in the volume of the remaining foci (Fig. 3D,E). We revealed a similar evolution for BRCA1 foci in Nup50-depleted cells, whereas Nup153- and Tpr-depleted cells showed a reduced number of BRCA1 foci with no increment in their volume (Fig. 3B,D), potentially due to impaired recruitment of BRCA1 to the break sites. 53BP1 foci were formed within the first 2 h after DNA damage induction in control and nucleoporin-depleted cells (Fig. 3C), which, in contrast to in control cells, remained constant in number (Fig. 3B) and volume (Fig. 3E) in the depleted cells, which might be due to inefficient replenishment of 53BP1 to the damaged sites resulting in an inefficient dissolution of the 53BP1 repair foci.

Sumoylation of 53BP1 is impaired upon Nup153 depletion

Previous work revealed that efficient accumulation of 53BP1 at sites of DSBs requires the E3 SUMO ligase PIAS4 and 53BP1 modification by SUMO1 (Galanty et al., 2009). We hypothesised that sumoylation of 53BP1 might be hampered in the absence of the nuclear basket components. To address this hypothesis, we treated U2OS cells stably expressing GFP–SUMO1, GFP–SUMO2 and

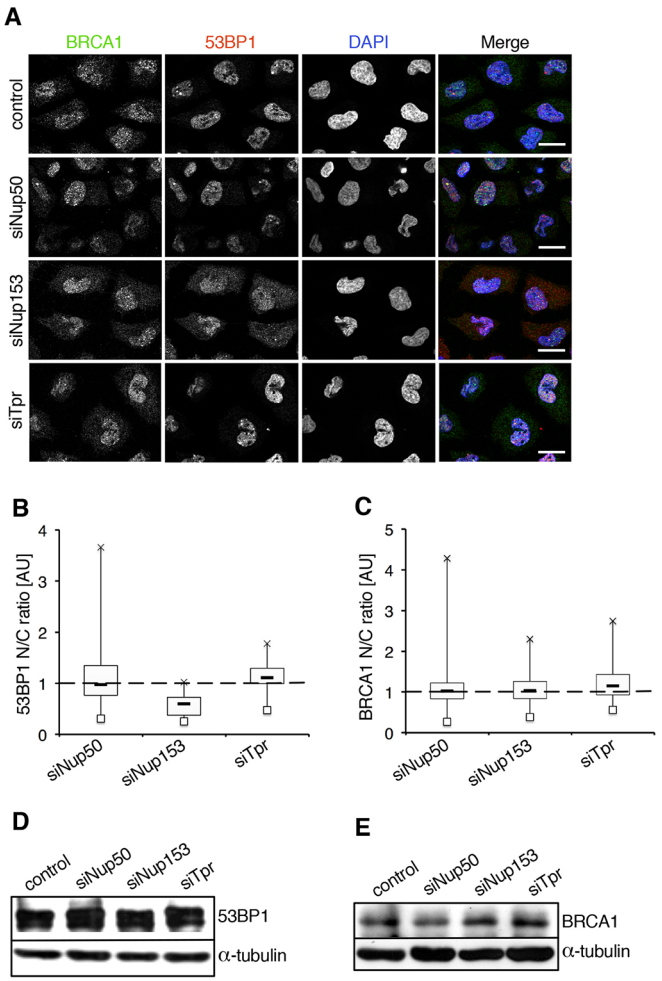

Fig. 2. Nuclear import of DSB repair factors is only moderately affected by depletion of NPC nuclear basket components. (A) Immunofluorescence analysis of 53BP1 and BRCA1 localisation in U2OS cells treated with the indicated siRNAs. Only Nup153-depleted cells showed partial 53BP1 re-localisation from the nucleus to the cytoplasm. BRCA1 is found primarily in the nucleus regardless of nucleoporin depletion. Cells were analysed by indirect immunofluorescence using anti-BRCA1 and anti-53BP1 antibodies. DNA was visualised by DAPI staining. Shown are confocal images. Scale bars: 10 µm. Quantification of the nuclear to cytoplasmic (N/C) distribution of (B) 53BP1 and (C) BRCA1 in U2OS cells treated with the indicated siRNAs. Nuclear and cytoplasmic fluorescence intensity was quantified for 40 cells from at least three independent experiments. The box plots represent the 25–75th percentiles, and the median is indicated. Whiskers show 1.5× the interquartile range above or below the data. Outliers are not shown. Western blot analysis of U2OS cellular extracts revealed that the expression levels of (D) 53BP1 and (E) BRCA1 remained unaffected by the depletion of nuclear basket components from NPCs when compared to α-tubulin. AU, arbitrary units.

Journal of Cell Science (2017) 130, 2306-2316 doi:10.1242/jcs.198390

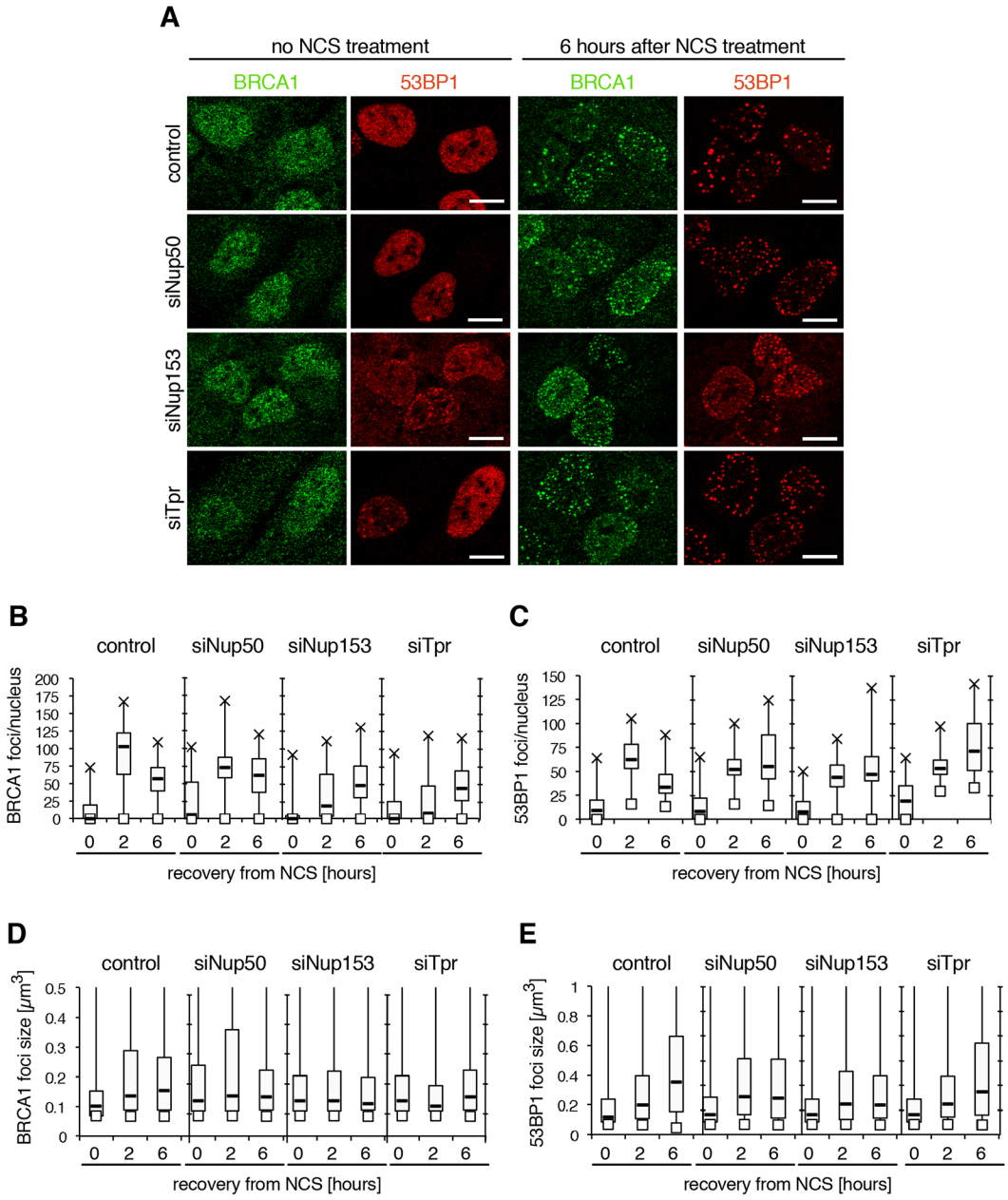

Fig. 3. DNA DSB repair is delayed in cells lacking nuclear basket nucleoporins. U2OS cells were treated with indicated siRNAs for 3 days and exposed to 50 ng/ml NCS for 15 min. At indicated times, cells were (A) co-immunostained for BRCA1 and 53BP1. Shown are representative confocal images. Quantification of (B) BRCA1 and (C) 53BP1 foci number as well as (D) BRCA1 and (E) 53BP1 foci size. A total of at least 50 cells were analysed per time point from three independent experiments. The box plots represent the 25–75th percentiles, and the median is indicated. Whiskers show 1.5× the interquartile range above or below the data. Outliers are not shown.

GFP–SUMO3, respectively (Galanty et al., 2009), with NCS and carried out colocalisation experiments analysing the particular SUMO forms and 53BP1. We confirmed that, upon DSB induction, 53BP1 colocalised with SUMO1, but not SUMO2 and SUMO3 (Fig. 4A). Similar results were obtained with NCS-treated HeLa cells stably expressing YFP–SUMO1 (Fig. S1C). We next transiently transfected the GFP–SUMO cell lines with an N-terminally HA-tagged 53BP1 (HA–53BP1). Western blot analysis revealed that, in U2OS cells treated with NCS, HA–53BP1 is sumoylated by GFP–SUMO1, but not by GFP–SUMO2 and GFP–SUMO3 (Fig. 4B). Co-expression of the SUMO-isopeptidase SENP1 with HA–53BP1 in the GFP–SUMO1-expressing U2OS cells prevented the appearance of the modified HA–53BP1 upon NCS-mediated DSB induction, confirming that 53BP1 is indeed modified by SUMO1 (Fig. 4C). Upon the respective depletion of Nup153, Nup50 and Tpr, we found that the association of GFP–SUMO1 with 53BP1 was reduced in U2OS cells depleted for Nup153, but increased in the absence of Tpr (Fig. 4D–G), indicating that altered sumoylation of 53BP1 might indeed account for the defects in NHEJ in these cells. Downregulation of Nup50, in contrast, had no effect on the association of GFP–SUMO1 with 53BP1 (Fig. 4D–G). The role of Tpr for protein sumoylation appears to be more general, whereas Nup153 appears to be specifically required for SUMO1 modification of 53BP1; cells depleted for Tpr exhibited a significant increase in global SUMO1 and SUMO2 modification of proteins, whereas global SUMO

Journal of Cell Science (2017) 130, 2306-2316 doi:10.1242/jcs.198390

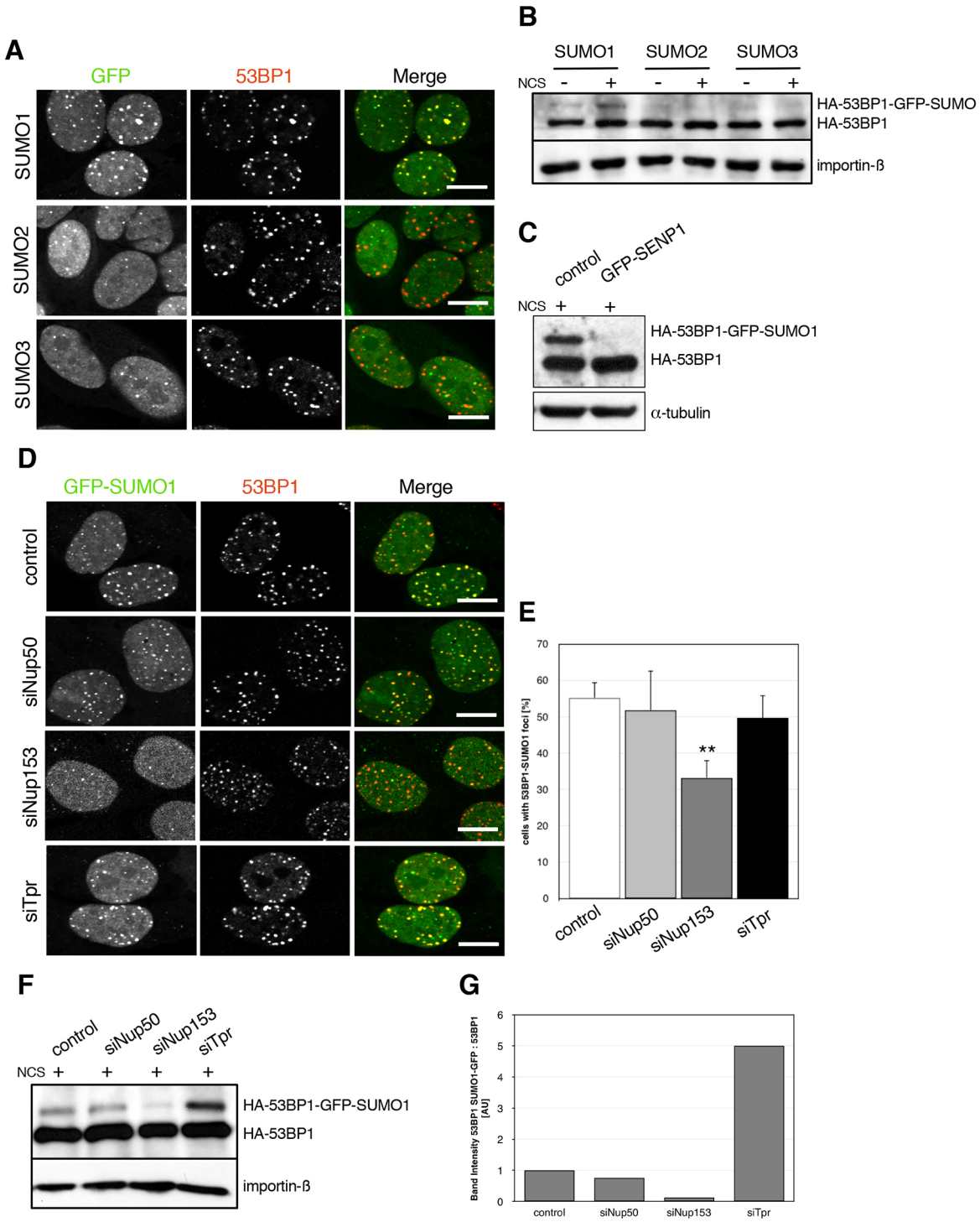

Fig. 4. Nup153 and Tpr affect the SUMO-1 modification of 53BP1. U2OS cells stably expressing GFP-tagged SUMO1, SUMO2 and SUMO3, respectively, were treated with NCS to induce DNA DSBs and (A) stained for 53BP1. Analysis by fluorescence confocal microscopy revealed that GFP–SUMO1 colocalised with 53BP1 foci, in contrast to GFP–SUMO2 and GFP–SUMO3. (B) The GFP–SUMO U2OS lines were transiently transfected to express a HA-tagged version of 53BP1 and subjected to co-immunoprecipitation assays using anti-HA antibodies. Only GFP–SUMO1 associated with HA–53BP1. Anti-importin-β antibodies were used as the loading control. (C) The association of GFP–SUMO1 with HA–53BP1 was abolished by co-transfection with the GFP-tagged SUMO isopeptidase SENP1. Antibodies against α-tubulin were used to monitor equal loading. (D) U2OS cells stably expressing GFP–SUMO1 were incubated with the indicated siRNAs for 3 days, subjected to NCS treatment and stained with anti-53BP1 antibodies. Analysis by confocal microscopy revealed that colocalisation of GFP–SUMO1 with 53BP1 is altered in cells depleted for Nup153 and Tpr, but not in control and Nup50-depleted cells. Scale bars: 10 µm. (E) Quantification of the number of U2OS cells showing GFP–SUMO1-modified 53BP1 foci after transfection with the respective indicated siRNAs and treatment with NCS. 100–200 transfected cells from three independent experiments for each condition were analysed. Data present mean±s.e.m. $^{**}P<0.01$ (*t*-test, one-tailed). (F) Immunoblot analysis of GFP–SUMO1-expressing U2OS cells co-transfected with the indicated siRNAs and HA–53BP1 showed that Nup153 depletion lead to a decrease in SUMO1-modification of HA–53BP1, whereas the pool of modified 53BP1 increased in the absence of Tpr. Anti-importin-β antibodies were used as loading control. (G) Quantification of band intensities of HA–53BP1–GFP–SUMO1 normalised to HA–53BP1. Quantification was carried out on a lower, non-overexposed film shown in F. AU, arbitrary units.

Journal of Cell Science (2017) 130, 2306-2316 doi:10.1242/jcs.198390

profiles remained unchanged in the respective absence of Nup153 and Nup50 (Fig. S2). Sumoylation takes place in a cascade of three enzymatic steps, of which the third step comprises the actual transfer of SUMO to its target protein by an E3-SUMO ligase. The E3 SUMO ligase for 53BP1 is PIAS4, and it is in fact required for 53BP1 recruitment to DSB sites (Galanty et al., 2009). We therefore tested whether PIAS4 localisation and/or expression is altered in the absence of Nup153, but observed no difference in PIAS4 nuclear localisation and expression levels upon depletion of Nup153, consistent with an apparently proper 53BP1 recruitment to DSBs (Fig. S3). Likewise, the nuclear import and expression levels of PIAS1, another E3 SUMO ligase known to be critical for proper DSB repair (Galanty et al., 2009; Ishiai et al., 2004; Zlatanou and Stewart, 2010), remained unaffected by Nup153 depletion (Fig. S3). Moreover, overexpressed mCherry-tagged versions of PIAS1, PIAS2, PIAS3 and PIAS4 localised to the nucleus in NCS-treated and Nup153-depleted cells in a manner that was indistinguishable from that seen in control cells (Fig. S4).

SENP1 is partially displaced in the respective absence of Nup153 and Tpr

Two SUMO proteases, SENP1 and SENP2, are known to localise to the nuclear periphery, and Nup153 is involved in their recruitment (Chow et al., 2012, 2014; Cubenas-Potts et al., 2013; Hang and Dasso, 2002; Zhang et al., 2002). Delocalisation of Ulp1, the yeast homologue of SENP1 and SENP2, from NPCs caused increased DNA damage sensitivity and cell cycle defects (Lewis et al., 2007; Palancade et al., 2007; Zhao et al., 2004). We considered it possible that 53BP1 sumoylation is impaired in Nup153-depleted cells due to a displacement of SENP1 and/or SENP2 from NPCs. We therefore analysed the effect of Nup153 depletion on the localisation of SENP1 and SENP2, respectively. Detection of SENP1 by immunofluorescence microscopy revealed that SENP1 was enriched at the nuclear envelope (NE) in control and Nup50-depleted cells, whereas it was reduced at the NE and partially displaced to the cytoplasm in Nup153- as well as Tpr-depleted cells (Fig. 5A,B). Consistent with the redistribution of SENP1 in cells lacking Nup153 or Tpr, the relative fluorescence intensity at the NE decreased by ∼40% in Nup153-depleted cells and 30% in Tpr-depleted cells (Fig. 5C). Western blot analysis of U2OS lysates revealed that SENP1 levels were lowered in cells lacking Nup153 (Fig. 5D; see also Fig. S5A for control of SENP1 depletion by siRNAs directed against SENP1), as previously described (Chow et al., 2014). In addition, in Tpr-depleted, but not in control or Nup50-depleted cells, relative levels of SENP1 were reduced (Fig. 5E). In contrast to SENP1, SENP2 expression remained unaffected by depletion of the nuclear basket nucleoporins (Fig. S5B; see also Fig. S5A for control of SENP2 depletion by siRNAs directed against SENP2). Owing to the fact that antibodies were largely inadequate for immunofluorescence, potential changes in SENP2 localisation could not be monitored (data not shown).

Tethering of SENP1 to the NPC protects cells against deficiencies in DNA damage response

In order to confirm that the loss of SENP1 from the NE contributes to the defects in DSB repair observed in cells lacking Nup153 or Tpr, we next tethered SENP1 artificially to the NPC. Specifically, we fused the N-terminal domain of Nup153, which contains its

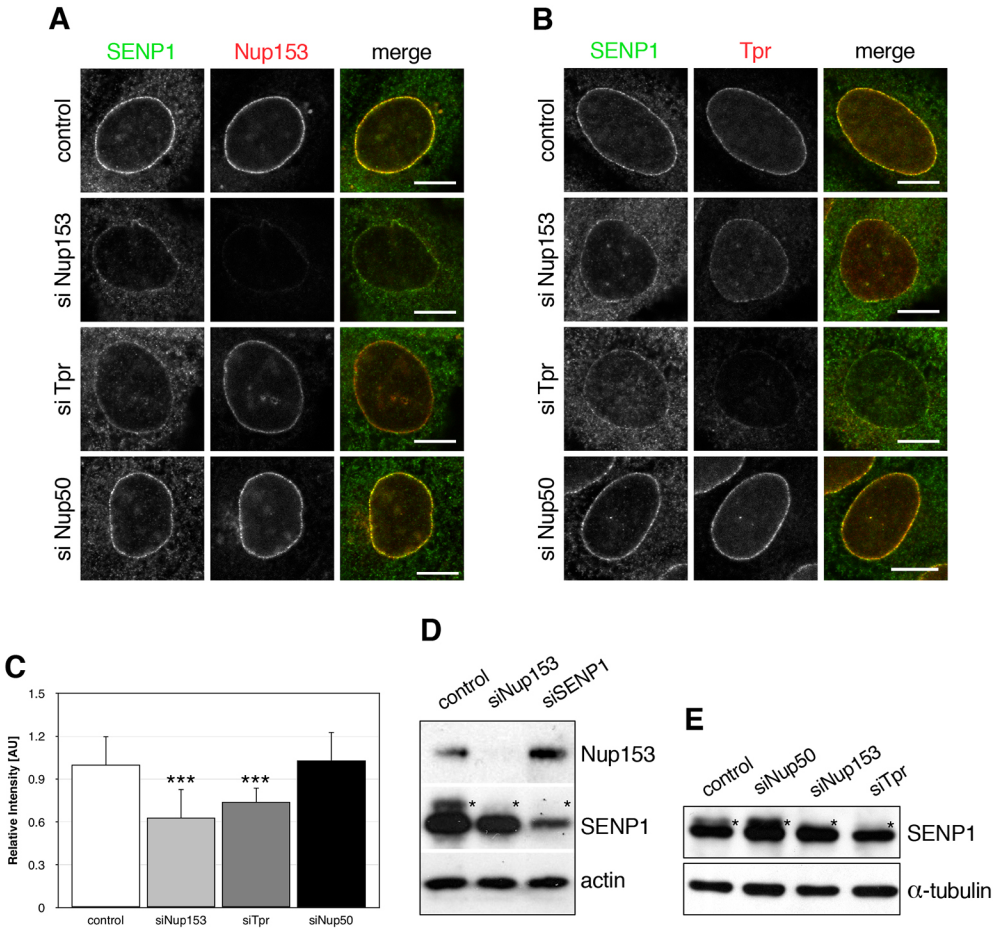

Fig. 5. SENP1 nuclear envelope localisation depends on Nup153 and Tpr. (A,B) SENP1 is enriched at NPCs in control and Nup50-depleted U2OS cells, but was partially re-localised to the cytoplasm in Nup153- and Tpr-depleted cells. Cells were analysed by indirect immunofluorescence microscopy. Shown are confocal sections on the midplane of the nuclear envelope. Scale bars: 10 µm. (C) Quantification of the fluorescence intensity of SENP1 staining at NPCs. Intensities were measured on 60–70 transfected cells from three independent experiments for each condition and are mean±s.d. ***P<0.001 (t-test, one-tailed). (D) U2OS cells were treated with the indicated siRNAs for 3 days and cellular lysates were subjected to western blot analysis using antibodies against Nup153, SENP1 and actin as well as (E) SENP1 and α-tubulin. Reduced SENP1 expression levels were observed in Nup153- and Tpr-depleted cells as well as in SENP1-depleted cells. The asterisks indicate potentially SUMO-modified SENP1 (Bailey and O'Hare, 2004).

Journal of Cell Science

Journal of Cell Science (2017) 130, 2306-2316 doi:10.1242/jcs.198390

NPC-targeting domain (Ball and Ullman, 2005), to SENP1 (Nup153–SENP1; Fig. 6A). This fusion protein is resistant to siRNAs directed against the C-terminal region of Nup153 (Fig. 6B). Nup153–SENP1 localised to NPCs in transiently transfected U2OS cells treated beforehand with non-targeting siRNAs as well as siRNAs against Nup153 and Tpr (Fig. 6C).

To characterise the effect on DSB repair of artificially tethering SENP1 to NPCs, we next monitored the efficiency of NHEJ and HR

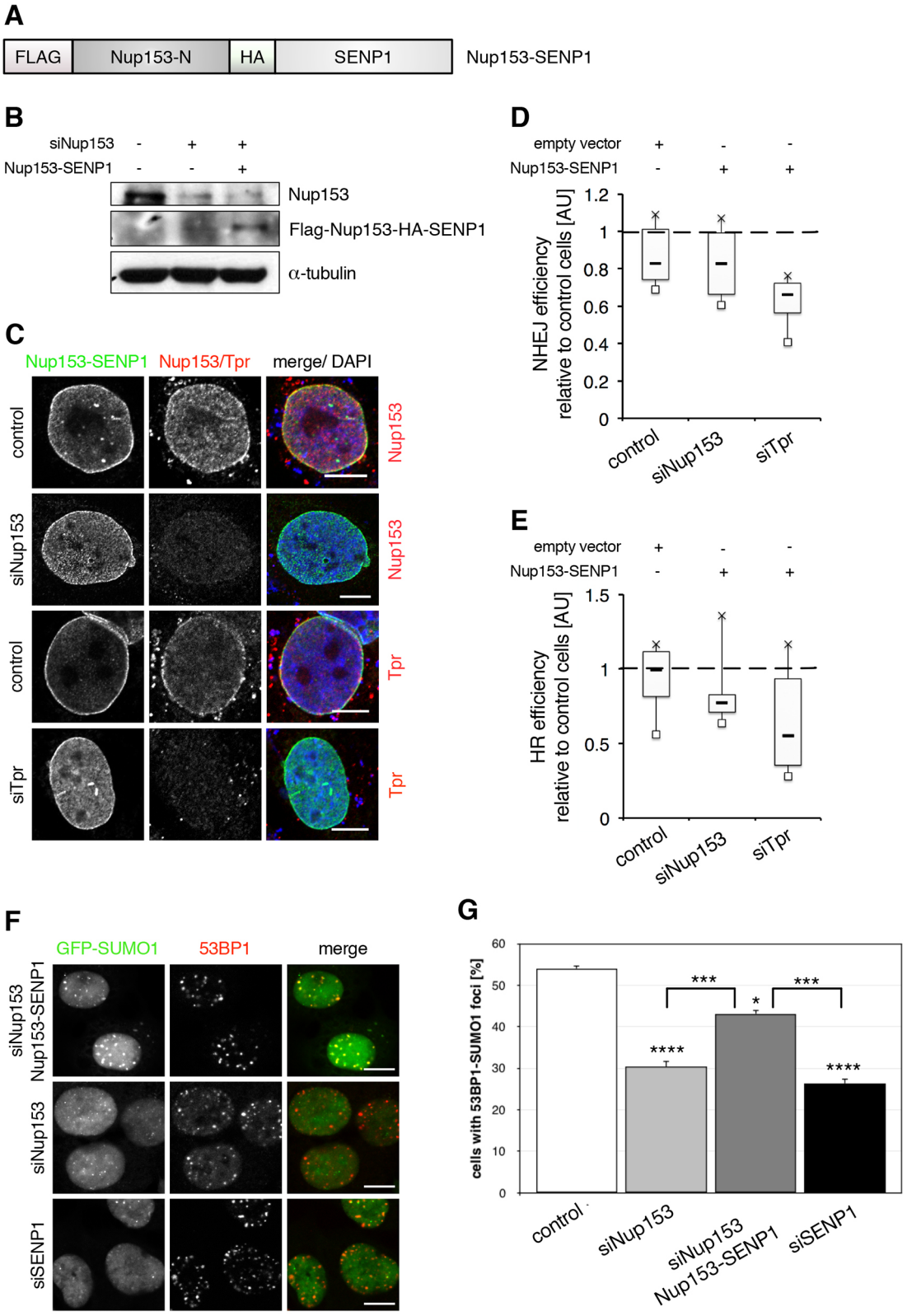

Fig. 6. See next page for legend.

Journal of Cell Science (2017) 130, 2306-2316 doi:10.1242/jcs.198390

Fig. 6. Artificial tethering of SENP1 partially restores DSB repair efficiency and 53BP1 sumoylation in Nup153-depleted cells. (A) Schematic diagram showing FLAG- and HA-tagged Nup153-N (residues 1–656) and SENP1 fusion protein. (B) U2OS cells were transfected with siRNAs against Nup153 and the fusion construct as indicated. Cell lysates were analysed by immunoblot using antibodies against Nup153, the FLAG tag and α-tubulin. (C) The Nup153–SENP1 fusion protein localised to NPCs in U2OS cells depleted for Nup153 or Tpr, similar to what was seen in control cells. Cells were analysed by indirect immunofluorescence microscopy using antibodies against Nup153 and Tpr as indicated. DNA was visualised by DAPI. Shown are confocal sections on the midplane of the nuclear envelope. Scale bars: 5 µm. Artificial tethering of SENP1 to NPCs (D) restored NHEJ efficiency in Nup153-depleted, but not in Tpr-depleted cells, whereas (E) HR efficiency was only partially rescued. NHEJ and HR efficiency for nucleoporin-depleted cells was quantified relative to control cells transfected with the Nup153–SENP1 fusion construct (value set at 1) for 50,000 cells per condition from three independent experiments. The box plots in D and E represent the 25–75th percentiles, and the median is indicated. Whiskers show 1.5× the interquartile range above or below the data. Outliers are not shown. (F) U2OS cells were transfected with siRNAs against Nup153 and the fusion construct as indicated, treated with NCS to induce DNA DSBs and stained for 53BP1. Shown are representative confocal images. Scale bars: 10 µm. (G) Quantification of the number of U2OS cells showing GFP–SUMO1-modified 53BP1 foci after transfection with siRNAs against Nup153 and the fusion construct as indicated and treatment with NCS. 100–200 transfected cells from three independent experiments for each condition were analysed. Data present mean±s.e.m. ****P<0.0001; ***P<0.001; *P<0.05 (t-test, one-tailed).

using the reporter constructs outlined above. U2OS cells were first treated with the experimental siRNAs for 72 h, and subsequently co-transfected with Nup153–SENP1 and the respective reporter constructs for NHEJ and HR. After a further 24 h, NHEJ and HR efficiency were each analysed by flow cytometry. As shown in Fig. 6D, artificial tethering of SENP1 to NPCs could rescue NHEJ efficiency in cells lacking Nup153, but not in cells lacking Tpr (see also Fig. 1B). NHEJ efficiency of Nup153-depleted cells with tethered SENP1 was similar to that of cells treated with non-targeting siRNAs expressing only endogenous SENP1. Tethering SENP1 to NPCs in the control cells further enhanced the efficiency of NHEJ (defined as value 1). In contrast to NHEJ, artificial tethering of SENP1 to NPCs could only partially rescue HR deficiency in Nup153-depleted cells as compared to control cells expressing endogenous SENP1 or tethered SENP1, while again HR deficiency could not be rescued in Tpr-depleted cells (Figs 6E and 1C).

To confirm that the displacement of SENP1 and the defects in NHEJ in Nup153-depleted cells are in fact due to impaired sumoylation of 53BP1, we next tested whether artificial tethering of SENP1 to NPCs also rescues the reduced association of GFP–SUMO1 with 53BP1 as seen in Nup153-depleted cells (Fig. 4D), although it is somewhat counter-intuitive that a SUMO protease would promote SUMO modification of 53BP1. As shown in Fig. 6F, alongside the quantification in Fig. 6G, Nup153-depleted cells with tethered SENP1 showed an accumulation of GFP–SUMO1 at 53BP1 foci in U2OS cells treated with NCS that was comparable to that in control cells, in contrast to Nup153-depleted cells and SENP1-depleted cells. SENP1 depletion, in contrast to Nup153 depletion, did not affect nuclear import of 53BP1 (and BRCA1, Fig. S5C,D). As seen for Nup153, depletion of SENP1 does not compromise the localisation and expression of the two E3 SUMO ligases PIAS1 and PIAS4 (Fig. S3) nor the localisation of over-expressed mCherry-tagged versions of PIAS1–PIAS4 (Fig. S4). Taken together, our data indicate that defects in NHEJ, but not in HR, in Nup153-depleted cells are, at least in part, due to displacement of SENP1 from NPCs. Tpr acts in a manner that is unrelated to SENP1 localisation at NPCs, suggesting that Nup153 and Tpr have different and independent roles in DNA DSB repair.

DISCUSSION

Silencing Nup153 compromises SUMO1 modification of 53BP1

The results of this study broaden the spectrum of the function of Nup153 in the maintenance of genome integrity. Previous studies have shown that Nup153 is important for the nuclear import of 53BP1 and efficient NHEJ (Lemaitre et al., 2012; Moudry et al., 2011). By carrying out a more systematic analysis of the function of Nup153 in the DDR, we demonstrate here that Nup153 is similarly required for the sumoylation of 53BP1. We observed no impaired recruitment of 53BP1 to DSBs, but decreased growth of repair foci and their delayed dissolution (Fig. 3). Efficient accumulation of 53BP1 at repair sites requires its modification by SUMO1 (Galanty et al., 2009), and SUMO pathway components are often associated with nuclear pores (for reviews, see Palancade and Doye, 2008; Rodriguez, 2014). While 53BP1 and SUMO1 largely colocalised at repair foci in control cells, this was diminished in Nup153-depleted U2OS cells, but not in Tpr- or Nup50-depleted cells (Fig. 4). This reduced sumoylation of 53BP1 was not provoked by impaired nuclear import of PIAS4, the E3 SUMO ligase promoting SUMO1 modification of 53BP1 (Galanty et al., 2009), but rather by a displacement of the SUMO protease SENP1 from NPCs in the absence of Nup153 (Fig. 5; Fig. S3). Artificial tethering of SENP1 to NPCs restored NHEJ efficiency and 53BP1 sumoylation after silencing of Nup153 (Fig. 6). It is somewhat counter-intuitive that a SUMO protease promotes SUMO modification of 53BP1, but similar observations have been made in fission yeast, where the deletion of Nup132, the *Schizosaccharomyces pombe* homologue of human Nup133, caused delocalisation of Ulp1 from NPCs, leading to DNA damage and cell cycle defects (Nie and Boddy, 2015). These defects were thought to arise from inappropriate desumoylation of nucleoplasmic targets that are normally spatially protected from Ulp1. Delocalised Ulp1 allowed an accumulation of SUMO chains on Pli1, a PIAS family SUMO E3 ligase and the *S. pombe* homologue of PIAS1, and its targeting for proteosomal degradation, which resulted in profound SUMO pathway and cell cycle defects (Nie and Boddy, 2015). It will be interesting to see whether a similar crosstalk between sumoylation and ubiquitylation of a PIAS family or another SUMO E3 ligase contributes to the defects in DDR seen in Nup153-depleted cells. PIAS1 and PIAS4, the two most obvious candidates in the context of 53BP1 and DSB repair, appear, however, unaffected in cells lacking Nup153 (Figs S3 and S4); we observed no changes in their intracellular localisation or stability. Nevertheless, the notion that the balance between sumoylation and desumoylation of SUMO E3 ligases contributes to effective DSB repair is further supported by our observation that depletion of Tpr led to defects in NHEJ, to displacement of SENP1 from NPCs and to an increase in 53BP1 sumoylation (Figs 1–4). This increase in 53BP1 sumoylation in the absence of Tpr likely arises because of the impact of Tpr on the level and function of SENP2 (David-Watine, 2011; Xu et al., 2007). Which other components of the SUMO pathway, and potentially the ubiquitin pathway, are out of balance in Nup153- and Tpr-depleted cells is an interesting question to address in the future. It will be furthermore interesting to see whether our observations made here hold true in non-immortalised cells and for endogenous 53BP1. However, endogenous sumoylation of proteins is challenging to detect due to the dynamic nature of the modification and its low steady-state levels (see, for example, Becker et al., 2013).

Journal of Cell Science (2017) 130, 2306-2316 doi:10.1242/jcs.198390

Nup153 and HR-mediated repair

We observed here that silencing Nup153 sensitised U2OS cells to treatment with the radiomimetic drug NCS, which coincided with a decrease in cell viability as well as in NHEJ and HR (Fig. 1). In contrast to a previous study (Lemaitre et al., 2012), we noticed no shift from NHEJ to HR in Nup153-depleted cells. This discrepancy might arise from the different cell lines that were used; U2OS cells in our study and the human fibroblast line GC92 in the previous study (Lemaitre et al., 2012; Mamouni et al., 2014; Rass et al., 2009). Our data are, however, consistent with the fact that 53BP1 promotes the fidelity of homology-directed DNA repair (Ochs et al., 2016). Silencing or exhausting 53BP1 results in a switch from the usage of RAD51 as recombinase in HR to usage of RAD52, which translates into a shift from error-free repair to the mutagenic single-strand annealing pathway (Ochs et al., 2016). One prerequisite for the loading of RAD51 on damaged DNA is, among others, the recruitment of BCRA1, a key factor in HR (Daley and Sung, 2014). We observed a reduced number of BRCA1 foci with no increase in their volume after silencing of Nup153 (Fig. 3A), which would be consistent with defects in RAD51 loading to damage sites. For future studies, it will therefore be interesting to deepen the analysis of the impact of Nup153 on RAD51-dependent HR.

Other nuclear basket nucleoporins and DDR

Our study further revealed that the two other components of the NPC nuclear basket, Tpr and Nup50, both somewhat contribute to effective DSB repair, but that their respective depletion did not inhibit the nuclear import of 53BP1 (Fig. 3A). We found that rather than a decrease, there was in fact an increase in overall level of sumoylation in Tpr-depleted cells, in contrast to a previous study (David-Watine, 2011), which might be attributed to the different cell lines used (HeLa versus U2OS). Tpr-depleted cells also showed an increase in sumoylation of 53BP1 and a partial displacement of SENP1 from NPCs, but defects in NHEJ in the absence of Tpr could not be restored by artificially tethering SENP1 to NPCs (Fig. 6). The role of Tpr and Nup50 hence needs to be further elucidated, but might be linked to repair at telomeres, as seen in yeast; Nup60 in yeast, the homologue of Nup50, is involved in anchoring Ulp1 to NPCs, similar to Mlp1 and Mlp2, the two yeast homologues of Tpr (Palancade et al., 2007). There, the displacement of Ulp1 from NPCs affected sumoylation of yKu70, a key player in NHEJ. In *mlp1/mlp2* mutants, it was shown that yKu70 function is impaired in DNA repair at telomeres (Hediger et al., 2002). It will therefore be interesting to see whether Tpr and Nup50 are also involved in NHEJ at telomeres in human cells. Tpr is furthermore phosphorylated upon DNA damage by the ATM/ATR kinases and involved in the proper activation of G2/M and intra-S check point (Matsuoka et al., 2007). If and how this might be linked to our observations here remains a subject for future studies.

MATERIALS AND METHODS

All experiments were carried out at room temperature (RT) unless otherwise stated.

Cell lines and transfections

All experiments were conducted in U2OS cells (a kind gift from Dr Harald Herrmann, German Cancer Research Center, Heidelberg, Germany; tested for contamination, but not authenticated) grown in Dulbecco's modified Eagle's medium (DMEM), supplemented with 10% fetal bovine serum (FBS) plus penicillin and streptomycin. Cells were transfected with plasmids by using the Turbofect transfection reagent (Thermo Scientific Fermentas, St. Leon-Rot, Germany) and with siRNAs by using Lipofectamine RNAiMAX (Life Technologies Invitrogen, Ghent, Belgium) following the instructions of the manufacturer. Smart-pool small interfering RNAs were obtained from Dharmacon (GE Healthcare Europe, Diegem, Belgium) as follows: Nup50 (L-012369-01), Nup153 (L-005283-00), Tpr (L-010548-00), 53BP1 (L-003548-00), Rad51 (L-003530-00), SENP1 (L-006357-00-0005), SENP2 (L-006033-00-0005) and non-targeting siRNAs (D-001810-10).

Plasmids and stable cell lines

U2OS cell lines (not tested and not authenticated) expressing SUMO1–GFP, SUMO2–GFP and SUMO3-GFP were a gift from Dr Steve Jackson (University of Cambridge, Cambridge, UK); HeLa cells expressing YFP–SUMO1 were a gift from Dr Angus Lamond (University of Dundee, Dundee, UK), pDRGFP and pCBASCeI were from Addgene [Addgene plasmids 26475 (Pierce et al., 1999) and 26477 (Richardson et al., 1998), deposited by Maria Jasin], pEGFP-Pem1-Ad2 and pDsRed2-N1 were kindly provided by Dr Vera Gorbunova (University of Rochester, NY), pEGFP-SENP1 by Dr Mary Dasso (NIH, Bethesda, USA), pmCherry-PIAS constructs were received from Dr Simon E. Fisher (Radboud University, Nijmegen, The Netherlands) and pCMH6K53BP1 (HA-53BP1) was a gift from Dr Aidan Doherty (University of Sussex, Brighton, UK).

For the generation of pcDNA3.1-FLAG-Nup153-HA-SENP1, SENP1 was PCR amplified and subcloned from pEGFP-SENP1 into KpnI- and NotI-cut pcDNA3.1-myc-His (reading frame B; Invitrogen, Carlsbad, CA), thereby integrating a HA tag, with the forward primer (5′-GGGGT-ACCATGTACCCATACGATGTTCCAGATTACGCTGATGATATTGCT-GATAGG-3′) and a STOP codon with the reverse primer (5′-ATAAGAATGCGGCCGCTCACAAGAGTTTTCGGTG-3′) to result in pcDNA3.1-HA-SENP1. Nup153 nucleotides 1–1968 (amino acids 1–656) were amplified by a PCR and subcloned from pEGFP-Nup153 (Fahrenkrog et al., 2002) into HindIII- and KpnI-cut pcDNA3.1-HA-SENP1. A FLAG tag was thereby integrated into the forward primer (5′-CCCAAGCTTATGGACTACAAAGACGATGACGACAAGGCCTCGG-GAGCCGGA-3′), the reverse primer was (5′-GGGGTACCTAAACTCT-CCCCAAACCC-3′). In-frame insertion was confirmed by DNA sequencing.

Antibodies

The following antibodies were used: polyclonal rabbit anti-53BP1 [Santa Cruz Biotechnology sc-22760; lot I-1813; immunofluorescence (IF) 1:500; western blotting (WB) 1:1000], rabbit anti-α-tubulin (Abcam ab18251; lot GR52624-1; WB 1:2000), rabbit ant-importin-β (kind gift of Ralph Kehlenbach, University of Göttingen, Germany; WB 1:1000), rabbit anti-SENP1 (Abcam ab108981; lot YG102603C; IF 1:1500; WB 1:1000), rabbit anti-Nup50 (Abgent AP1913b; lot SH05120G; IF 1:1000; WB 1:250), rabbit anti-SENP2 (kind gift of Michael Matunis, Johns Hopkins Bloomberg School of Public Health, MD; IF 1:50; WB 1:500), rabbit anti-SENP2 (Santa Cruz Biotechnology, sc-67075; IF: 1:50; lot H-1813), as well as monoclonal mouse anti-BRCA1 (Santa Cruz Biotechnology sc-6954; lot D1713; IF 1:1000; WB 1:1000), mouse anti-HA (hybridoma supernatant; WB 1:50), mouse anti-Nup153 (SA1; hybridoma supernatant; IF 1:800; WB 1:200), mouse monoclonal anti-Tpr (Abnova H00007175-M01; lot 10131-1A8; IF 1:6000; WB 1:2000), mouse anti-FLAG (Sigma-Aldrich F-3165; lot 087K6002V; IF: 1:200), and rat anti-GFP (Chromotek, clone 3H9; lot 130624; WB 1:1000).

Clonogenic survival assay

U2OS were treated with siRNAs for 72 h, trypsinised, stained with Trypan Blue solution according to the manufacturer's instructions (Sigma-Aldrich, Diegem, Belgium) and counted using a haemocytometer. 1000 cells were seeded per well of a 6-well plate and grown for 12–14 h. Next, cells were treated with neocarzinostatin (NCS; Sigma-Aldrich, Diegem, Belgium) with doses ranging from 0 through 10 µg/ml for 15 min, washed extensively in PBS and released into fresh medium. Colonies were allowed to grow for 10 days, the wells were washed in PBS, fixed in 4% paraformaldehyde for 15 min, washed in PBS, stained with 0.5% Crystal Violet solution and colonies were counted manually. The surviving fractions were calculated and normalised to untreated control.

NHEJ assay

NHEJ fidelity was determined according to Seluanov et al. (2004). In brief, the pEGFP-Pem1-Ad2 reporter plasmid was linearised with I-SceI (New England Biolabs) and purified using a Qiagen gel extraction kit; complete digestion was confirmed by gel electrophoresis. U2OS cells were treated with siRNAs against the nuclear basket nucleoporins Nup153, Nup50 and Tpr, respectively, as well as scrambled siRNAs, for 72 h and next co-transfected with the linearised pEGFP-Pem1-Ad2 (to monitor NHEJ) and pDsRed2-N1 (to monitor transfection efficiency) (Seluanov et al., 2004). The cells were harvested 24 h after transfection, resuspended in 0.5 ml of PBS, and assayed for the expression of EGFP and DsRed by flow cytometry (FACS Calibur, BD Biosciences) according to the guidelines in Seluanov et al. (2004).

HR assay

HR efficiency was determined using U2OS cells stably expressing the integrated HR reporter DR-GFP (see above). Cells were transfected with siRNAs against the nuclear basket nucleoporins Nup153, Nup50, and Tpr, respectively, as well as scrambled siRNAs, for 40 h and next co-transfected with pCBA-I-SceI (to monitor HR) and pDsRed2-N1 (to monitor transfection efficiency). The cells were harvested at 48 h after plasmid transfection, resuspended in 0.5 ml of PBS, and assayed for the expression of EGFP and DsRed by flow cytometry according to Pierce et al. (1999).

Immunofluorescence

Cells were grown on coverslips, fixed in 4% paraformaldehyde for 15 min and permeabilised in Tris-buffered saline (TBS) containing 0.3% Triton X-100 for 5 min. After blocking for 60 min in TBS containing 5% BSA, cells were incubated with primary antibodies overnight at 4°C. Following washing steps, cells were incubated with fluorochrome-coupled secondary antibody for 45 min at RT and mounted in Mowiol 4-88 (Sigma) containing 1 µg/ml DAPI. Images were acquired with a Zeiss LSM 710 laser-scanning confocal microscope and the Zen system software. Images were processed using ImageJ and Adobe Photoshop.

Image J quantification

Quantification of western blots and immunofluorescence images were carried out following the same principles. In brief, areas of interest and background areas were delimited and their 'mean grey values' were measured using ImageJ. Values of background areas were subtracted from values of areas of interest and respective ratios were calculated.

Volumes and numbers of 53BP1 and BRCA1 foci were determined on confocal *Z*-stack pictures, using the '3D object counter' ImageJ plugin (https://imagej.nih.gov/ij/plugins/track/objects.html) according to the developer's guidelines (http://imagejdocu.tudor.lu/lib/exe/fetch.php?media=plugin:analysis:3d_object_counter:3d-oc.pdf; Bolte and Cordelieres, 2006).

Western blotting

U2OS cells were lysed in lysis buffer [50 mM Tris-HCl, pH 7.8, 150 mM NaCl, 1% Nonidet-P40 and protease inhibitor cocktail tablets (Roche, Basel Switzerland)]. In case of the GFP–SUMO-expressing U2OS lines, the lysis buffer additionally contained 20 mM N-ethylmaleimide (Sigma-Aldrich) to inhibit de-sumoylation. 20 µg of protein were loaded and separated by SDS-PAGE (5% or 7% gels). The proteins were transferred onto a PVDF membrane (Immobilon-P, Millipore) and the membranes were blocked with TBS containing 0.1% Tween 20 and 5% non-fat dry milk for 1 h. The membranes were then incubated for 1 h in blocking solution containing a primary antibody followed by washing 3× in TBS containing 0.1% Tween 20 and 5% non-fat dry milk. The membranes were next incubated with alkaline phosphatase-labelled secondary antibodies for 1 h, washed 3× in TBS and developed using Lightning CDP Star Chemiluminescence reagent (Applied Biosystem) and an X-ray film. Films were scanned and processed using ImageJ.

Acknowledgements

The authors thank Drs. Mary Dasso (NIH, Bethesda, USA), Simon E. Fisher (Radboud University, Nijmegen, The Netherlands), Harald Herrmann (German Cancer Research Center, Heidelberg), Maria Jasin (Memorial Sloan Kettering Cancer Center, New York, USA), Ralph Kehlenbach (University of Göttingen, Germany), Angus Lamond (University of Dundee, Scotland, UK), and Mike Matunis (Johns Hopkins University, Baltimore, USA) for sharing reagents. Ralph Kehlenbach is further acknowledged for critically reading the manuscript.

Competing interests

The authors declare no competing or financial interests.

Author contributions

Conceptualization: V.D., N.N., B.F.; Validation: V.D., N.N., S.P., V.M., B.F.; Formal analysis: V.D., N.N., B.F.; Investigation: V.D., N.N., S.P., V.M.; Writing - original draft: V.D., B.F.; Writing - review & editing: V.D., N.N., B.F.; Supervision: V.D., B.F.; Project administration: V.D., B.F.; Funding acquisition: B.F.

Funding

This work was supported by grants from the Fonds De La Recherche Scientifique - FNRS, Belgium (grant numbers 1.5091. 12 and T.0237.13, Télévie grants 7.4519.12F and 7.6534.16F), the Fédération Wallonie-Bruxelles (ARC 4.110. F.000092F), the Fonds Brachet, the Fonds Alice et David van Buuren, and by the Université Libre de Bruxelles, Belgium.

Supplementary information

Supplementary information available online at
http://jcs.biologists.org/lookup/doi/10.1242/jcs.198390.supplemental

References

Bailey, D. and O'Hare, P. (2004). Characterization of the localization and proteolytic activity of the SUMO-specific protease, SENP1. *J. Biol. Chem.* **279**, 692-703.

Ball, J. R. and Ullman, K. S. (2005). Versatility at the nuclear pore complex: lessons learned from the nucleoporin Nup153. *Chromosoma* **114**, 319-330.

Beck, M., Förster, F., Ecke, M., Plitzko, J. M., Melchior, F., Gerisch, G., Baumeister, W. and Medalia, O. (2004). Nuclear pore complex structure and dynamics revealed by cryoelectron tomography. *Science* **306**, 1387-1390.

Beck, M., Lučić, V., Förster, F., Baumeister, W. and Medalia, O. (2007). Snapshots of nuclear pore complexes in action captured by cryo-electron tomography. *Nature* **449**, 611-615.

Becker, J., Barysch, S. V., Karaca, S., Dittner, C., Hsiao, H.-H., Diaz, M. B., Herzig, S., Urlaub, H. and Melchior, F. (2013). Detecting endogenous SUMO targets in mammalian cells and tissues. *Nat. Struct. Mol. Biol.* **20**, 525-531.

Bogerd, A. M., Hoffman, J. A., Amberg, D. C., Fink, G. R. and Davis, L. I. (1994). nup1 mutants exhibit pleiotropic defects in nuclear pore complex function. *J. Cell Biol.* **127**, 319-332.

Bolte, S. and Cordelieres, F. P. (2006). A guided tour into subcellular colocalization analysis in light microscopy. *J. Microsc.* **224**, 213-232.

Chow, K.-H., Elgort, S., Dasso, M. and Ullman, K. S. (2012). Two distinct sites in Nup153 mediate interaction with the SUMO proteases SENP1 and SENP2. *Nucleus* **3**, 349-358.

Chow, K.-H., Elgort, S., Dasso, M., Powers, M. A. and Ullman, K. S. (2014). The SUMO proteases SENP1 and SENP2 play a critical role in nucleoporin homeostasis and nuclear pore complex function. *Mol. Biol. Cell* **25**, 160-168.

Cobb, A. M., Larrieu, D., Warren, D. T., Liu, Y., Srivastava, S., Smith, A. J. O., Bowater, R. P., Jackson, S. P. and Shanahan, C. M. (2016). Prelamin A impairs 53BP1 nuclear entry by mislocalizing NUP153 and disrupting the Ran gradient. *Aging Cell* **15**, 1039-1050.

Cronshaw, J. M., Krutchinsky, A. N., Zhang, W., Chait, B. T. and Matunis, M. J. (2002). Proteomic analysis of the mammalian nuclear pore complex. *J. Cell Biol.* **158**, 915-927.

Cubenas-Potts, C., Goeres, J. D. and Matunis, M. J. (2013). SENP1 and SENP2 affect spatial and temporal control of sumoylation in mitosis. *Mol. Biol. Cell* **24**, 3483-3495.

Daley, J. M. and Sung, P. (2014). 53BP1, BRCA1, and the choice between recombination and end joining at DNA double-strand breaks. *Mol. Cell. Biol.* **34**, 1380-1388.

David-Watine, B. (2011). Silencing nuclear pore protein Tpr elicits a senescent-like phenotype in cancer cells. *PLoS ONE* **6**, e22423.

De Souza, C. P., Hashmi, S. B., Nayak, T., Oakley, B. and Osmani, S. A. (2009). Mlp1 acts as a mitotic scaffold to spatially regulate spindle assembly checkpoint proteins in Aspergillus nidulans. *Mol. Biol. Cell* **20**, 2146-2159.

Dickmanns, A., Kehlenbach, R. H. and Fahrenkrog, B. (2015). Nuclear pore complexes and nucleocytoplasmic transport: from structure to function to disease. *Int Rev Cell Mol Biol* **320**, 171-233.

Dilworth, D. J., Suprapto, A., Padovan, J. C., Chait, B. T., Wozniak, R. W., Rout, M. P. and Aitchison, J. D. (2001). Nup2p dynamically associates with the distal regions of the yeast nuclear pore complex. *J. Cell Biol.* **153**, 1465-1478.

Dilworth, D. J., Tackett, A. J., Rogers, R. S., Yi, E. C., Christmas, R. H., Smith, J. J., Siegel, A. F., Chait, B. T., Wozniak, R. W. and Aitchison, J. D. (2005). The

mobile nucleoporin Nup2p and chromatin-bound Prp20p function in endogenous NPC-mediated transcriptional control. *J. Cell Biol.* **171**, 955-965.
Duheron, V., Chatel, G., Sauder, U., Oliveri, V. and Fahrenkrog, B. (2014). Structural characterization of altered nucleoporin Nup153 expression in human cells by thin-section electron microscopy. *Nucleus* **5**, 601-612.
Fahrenkrog, B. and Aebi, U. (2003). The nuclear pore complex: nucleocytoplasmic transport and beyond. *Nat. Rev. Mol. Cell Biol.* **4**, 757-766.
Fahrenkrog, B., Maco, B., Fager, A. M., Köser, J., Sauder, U., Ullman, K. S. and Aebi, U. (2002). Domain-specific antibodies reveal multiple-site topology of Nup153 within the nuclear pore complex. *J. Struct. Biol.* **140**, 254-267.
Flotho, A. and Melchior, F. (2013). Sumoylation: a regulatory protein modification in health and disease. *Annu. Rev. Biochem.* **82**, 357-385.
Frenkiel-Krispin, D., Maco, B., Aebi, U. and Medalia, O. (2010). Structural analysis of a metazoan nuclear pore complex reveals a fused concentric ring architecture. *J. Mol. Biol.* **395**, 578-586.
Galanty, Y., Belotserkovskaya, R., Coates, J., Polo, S., Miller, K. M. and Jackson, S. P. (2009). Mammalian SUMO E3-ligases PIAS1 and PIAS4 promote responses to DNA double-strand breaks. *Nature* **462**, 935-939.
Gay, S. and Foiani, M. (2015). Nuclear envelope and chromatin, lock and key of genome integrity. *Int Rev Cell Mol Biol* **317**, 267-330.
Géli, V. and Lisby, M. (2015). Recombinational DNA repair is regulated by compartmentalization of DNA lesions at the nuclear pore complex. *BioEssays* **37**, 1287-1292.
Gong, L., Millas, S., Maul, G. G. and Yeh, E. T. (2000). Differential regulation of sentrinized proteins by a novel sentrin-specific protease. *J. Biol. Chem.* **275**, 3355-3359.
Hang, J. and Dasso, M. (2002). Association of the human SUMO-1 protease SENP2 with the nuclear pore. *J. Biol. Chem.* **277**, 19961-19966.
Hediger, F., Dubrana, K. and Gasser, S. M. (2002). Myosin-like proteins 1 and 2 are not required for silencing or telomere anchoring, but act in the Tel1 pathway of telomere length control. *J. Struct. Biol.* **140**, 79-91.
Ibarra, A. and Hetzer, M. W. (2015). Nuclear pore proteins and the control of genome functions. *Genes Dev.* **29**, 337-349.
Ishiai, M., Kimura, M., Namikoshi, K., Yamazoe, M., Yamamoto, K., Arakawa, H., Agematsu, K., Matsushita, N., Takeda, S., Buerstedde, J. M. et al. (2004). DNA cross-link repair protein SNM1A interacts with PIAS1 in nuclear focus formation. *Mol. Cell. Biol.* **24**, 10733-10741.
Itahana, Y., Yeh, E. T. and Zhang, Y. (2006). Nucleocytoplasmic shuttling modulates activity and ubiquitination-dependent turnover of SUMO-specific protease 2. *Mol. Cell. Biol.* **26**, 4675-4689.
Kabachinski, G. and Schwartz, T. U. (2015). The nuclear pore complex–structure and function at a glance. *J. Cell Sci.* **128**, 423-429.
Kim, Y. H., Sung, K. S., Lee, S.-J., Kim, Y.-O., Choi, C. Y. and Kim, Y. (2005). Desumoylation of homeodomain-interacting protein kinase 2 (HIPK2) through the cytoplasmic-nuclear shuttling of the SUMO-specific protease SENP1. *FEBS Lett.* **579**, 6272-6278.
Kirby, T. W., Gassman, N. R., Smith, C. E., Pedersen, L. C., Gabel, S. A., Sobhany, M., Wilson, S. H. and London, R. E. (2015). Nuclear localization of the DNA repair scaffold XRCC1: uncovering the functional role of a bipartite NLS. *Sci. Rep.* **5**, 13405.
Kosova, B., Pante, N., Rollenhagen, C., Podtelejnikov, A., Mann, M., Aebi, U. and Hurt, E. (2000). Mlp2p, a component of nuclear pore attached intranuclear filaments, associates with nic96p. *J. Biol. Chem.* **275**, 343-350.
Lemaitre, C., Fischer, B., Kalousi, A., Hoffbeck, A. S., Guirouilh-Barbat, J., Shahar, O. D., Genet, D., Goldberg, M., Betrand, P., Lopez, B. et al. (2012). The nucleoporin 153, a novel factor in double-strand break repair and DNA damage response. *Oncogene* **31**, 4803-4809.
Lewis, A., Felberbaum, R. and Hochstrasser, M. (2007). A nuclear envelope protein linking nuclear pore basket assembly, SUMO protease regulation, and mRNA surveillance. *J. Cell Biol.* **178**, 813-827.
Lim, R. Y., Aebi, U. and Fahrenkrog, B. (2008). Towards reconciling structure and function in the nuclear pore complex. *Histochem. Cell Biol.* **129**, 105-116.
Maimon, T., Elad, N., Dahan, I. and Medalia, O. (2012). The human nuclear pore complex as revealed by cryo-electron tomography. *Structure* **20**, 998-1006.
Mamouni, K., Cristini, A., Guirouilh-Barbat, J., Monferran, S., Lemarié, A., Faye, J.-C., Lopez, B. S., Favre, G. and Sordet, O. (2014). RhoB promotes gammaH2AX dephosphorylation and DNA double-strand break repair. *Mol. Cell. Biol.* **34**, 3144-3155.
Matsuoka, S., Ballif, B. A., Smogorzewska, A., McDonald, E. R., III, Hurov, K. E., Luo, J., Bakalarski, C. E., Zhao, Z., Solimini, N., Lerenthal, Y. et al. (2007). ATM and ATR substrate analysis reveals extensive protein networks responsive to DNA damage. *Science* **316**, 1160-1166.
Moudry, P., Lukas, C., Macurek, L., Neumann, B., Heriche, J. K., Pepperkok, R., Ellenberg, J., Hodny, Z., Lukas, J. and Bartek, J. (2011). Nucleoporin NUP153 guards genome integrity by promoting nuclear import of 53BP1. *Cell Death Differ.* **19**, 798-807.
Mukhopadhyay, D. and Dasso, M. (2007). Modification in reverse: the SUMO proteases. *Trends Biochem. Sci.* **32**, 286-295.
Nie, M. and Boddy, M. N. (2015). Pli1(PIAS1) SUMO ligase protected by the nuclear pore-associated SUMO protease Ulp1SENP1/2. *J. Biol. Chem.* **290**, 22678-22685.
Ochs, F., Somyajit, K., Altmeyer, M., Rask, M.-B., Lukas, J. and Lukas, C. (2016). 53BP1 fosters fidelity of homology-directed DNA repair. *Nat. Struct. Mol. Biol.* **23**, 714-721.
Ori, A., Banterle, N., Iskar, M., Andres-Pons, A., Escher, C., Khanh Bui, H., Sparks, L., Solis-Mezarino, V., Rinner, O., Bork, P. et al. (2013). Cell type-specific nuclear pores: a case in point for context-dependent stoichiometry of molecular machines. *Mol. Syst. Biol.* **9**, 648.
Palancade, B. and Doye, V. (2008). Sumoylating and desumoylating enzymes at nuclear pores: underpinning their unexpected duties? *Trends Cell Biol.* **18**, 174-183.
Palancade, B., Liu, X., Garcia-Rubio, M., Aguilera, A., Zhao, X. and Doye, V. (2007). Nucleoporins prevent DNA damage accumulation by modulating Ulp1-dependent sumoylation processes. *Mol. Biol. Cell* **18**, 2912-2923.
Pierce, A. J., Johnson, R. D., Thompson, L. H. and Jasin, M. (1999). XRCC3 promotes homology-directed repair of DNA damage in mammalian cells. *Genes Dev.* **13**, 2633-2638.
Rass, E., Grabarz, A., Plo, I., Gautier, J., Bertrand, P. and Lopez, B. S. (2009). Role of Mre11 in chromosomal nonhomologous end joining in mammalian cells. *Nat. Struct. Mol. Biol.* **16**, 819-824.
Reichelt, R., Holzenburg, A., Buhle, E. L., Jr, Jarnik, M., Engel, A. and Aebi, U. (1990). Correlation between structure and mass distribution of the nuclear pore complex and of distinct pore complex components. *J. Cell Biol.* **110**, 883-894.
Richardson, C., Moynahan, M.E. and Jasin, M. (1998). Double-strand break repair by interchromosomal recombination: suppression of chromosomal translocations. *Genes Dev.* **12**, 3831-3842.
Rodríguez, J. A. (2014). Interplay between nuclear transport and ubiquitin/SUMO modifications in the regulation of cancer-related proteins. *Semin. Cancer Biol.* **27**, 11-19.
Rout, M. P., Aitchison, J. D., Suprapto, A., Hjertaas, K., Zhao, Y. and Chait, B. T. (2000). The yeast nuclear pore complex: composition, architecture, and transport mechanism. *J. Cell Biol.* **148**, 635-651.
Seluanov, A., Mittelman, D., Pereira-Smith, O. M., Wilson, J. H. and Gorbunova, V. (2004). DNA end joining becomes less efficient and more error-prone during cellular senescence. *Proc. Natl. Acad. Sci. USA* **101**, 7624-7629.
Strambio-de-Castillia, C., Blobel, G. and Rout, M. P. (1999). Proteins connecting the nuclear pore complex with the nuclear interior. *J. Cell Biol.* **144**, 839-855.
Xu, X. M., Rose, A., Muthuswamy, S., Jeong, S. Y., Venkatakrishnan, S., Zhao, Q. and Meier, I. (2007). NUCLEAR PORE ANCHOR, the Arabidopsis homolog of Tpr/Mlp1/Mlp2/megator, is involved in mRNA export and SUMO homeostasis and affects diverse aspects of plant development. *Plant Cell* **19**, 1537-1548.
Yeh, E. T. (2009). SUMOylation and De-SUMOylation: wrestling with life's processes. *J. Biol. Chem.* **284**, 8223-8227.
Zhang, H., Saitoh, H. and Matunis, M. J. (2002). Enzymes of the SUMO modification pathway localize to filaments of the nuclear pore complex. *Mol. Cell. Biol.* **22**, 6498-6508.
Zhao, X., Wu, C. Y. and Blobel, G. (2004). Mlp-dependent anchorage and stabilization of a desumoylating enzyme is required to prevent clonal lethality. *J. Cell Biol.* **167**, 605-611.
Zlatanou, A. and Stewart, G. S. (2010). A PIAS-ed view of DNA double strand break repair focuses on SUMO. *DNA Repair (Amst)* **9**, 588-592.